Supplementary Material

1. The updated data set

The raw data set consists of observed AAR (%) and mass balance ($\mathrm{kg\ m^{-2}\ yr^{-1}}$) for 144 GIC (125 glaciers and 19 ice caps) during 1971–2010. The data are tabulated in Sheet A (*AAR and mass balance*) of the Excel file, *Mernild_etal_TC.auxiliary_data.xls.* Most of the data are from a database established by the World Glacier Monitoring Service and described in published bulletins (WGMS, 2012). These data are listed without shading. The AAR values with grey shading are from Bahr et al. (2009), and the mass balance values with yellow shading are from Dyurgerov and Meier (2005). The data with blue shading were received from investigators during the preparation of this paper (see Sect. 12 of Supplementary Material). We found that the data set used by Bahr et al. (2009) generally omits AARs for glaciers with net ablation at all elevations (hence AAR=0) in a particular year. Including these values lowers the mean AAR. One glacier, Urumqihe S. No. 1, split into two branches in 1995. The AAR and mass balance from 1995 onward were derived by averaging observations from the two branches.

Based on Radić and Hock (2010), we divided the Earth's glaciated regions into eight high-mass regions (with an ice volume $V > 5{,}000\ \mathrm{km^3}$) and eight low-mass regions ($V < 5{,}000\ \mathrm{km^3}$); see Fig. 1 of the main text. The data set includes 38 GIC in high-mass regions (Arctic Canada, Antarctica, Alaska, Greenland, Russian Arctic, Central Asia, Svalbard, and Southern Andes) and 106 GIC in low-mass regions (Iceland, W. Canada/U.S., Northern Andes, Central Europe, Scandinavia, North Asia, Caucasus, and New Zealand).

2. Estimating $\mathbf{AAR_0}$

The computed values of AAR_0 were obtained by linear regression of AAR against mass balance, as illustrated in Fig. S1. These AAR_0 values are listed in Sheet B (*AAR_0 calculations*) along with r^2 for each linear regression (where r is the regression coefficient). Instances of $AAR = 0$ and $\mathrm{AAR} = 100\%$ were excluded from the regressions (but included for the broader analysis), since AAR and mass balance are not related linearly when net ablation occurs at all elevations or when net accumulation occurs at all elevations. The greater the number of observations, the smaller the value of r required for significance. The data set includes only GIC for which the linear relationship is significant at the 10% level or better, based on a linear regression t-test. The mean AAR_0 for the data set is 55 ± 2%, slightly below previous estimates of 58% from theory (Bahr et al., 1997) and $58 \pm 1\%$ from observations (Dyurgerov et al., 2009; Dyurgerov, 2010). Following Dyurgerov et al. (2009), we assumed that AAR_0 does not change in time.

3. Uncertainty ranges and significance levels

Uncertainties computed from our data set and stated in the text correspond to a 95% confidence interval, or 1.96 times the standard error. The computation of standard errors is described in detail below. Uncertainty ranges in other published work may not be directly comparable. BDM, for example, expressed uncertainties as plus or minus one standard error, corresponding to a 68% confidence interval. Thus the uncertainty ranges we computed are larger than the BDM ranges for two reasons: (1) the confidence interval is larger, and (2) we computed global uncertainties by propagating uncertainties from individual regions, as described below, whereas BDM assumed that their GIC sample was globally representative.

Trends labeled as significant are significant at the 1% level or better. Trends labeled insignificant do not pass any significance tests at a level of 10% of better. The term "likely" denotes 66–100% probability (Mastrandrea et al., 2010).

4. All GIC: alpha, p_A, p_V calculations

The first section of Sheet C (*All GIC – alpha, p_A, p_V*) shows values of $\alpha = \mathrm{AAR} / \mathrm{AAR}_0$ for the full data set. For each year *i*, the annual mean α is found by averaging over N_i values:

$$\overline{\alpha}_i = \frac{\sum_{n=1}^{N_i} \alpha_{ni}}{N_i}, \quad (1)$$

where α_{ni} denotes the value for glacier *n* in year *i*. The variance for each year is computed as

$$\sigma_i^2 = \frac{1}{N_i - 1} \sum_{n=1}^{N_i} (\alpha_{ni} - \overline{\alpha}_i)^2, \quad (2)$$

resulting in a standard error of

$$\delta\alpha_i = \frac{\sigma_i}{\sqrt{N_i}}. \quad (3)$$

The annual values and running 10-year means are shown in Fig. 3 of the main text.

Arithmetic means for the full data set were computed for four 10-year windows: 1971–1980, 1981–1990, 1991–2000, and 2001–2010. Decadal means $\overline{\alpha}_n$ for each glacier are shown in Sheet C. For the full data set we computed a mean α of 0.93 ± 0.06, 0.85 ± 0.06, 0.83 ± 0.07, and 0.59 ± 0.05 during the 1970s, 1980s, 1990s, and 2000s, respectively. Suppose that for a given glacier *n*, we have measurements in M_n out of 10 years ($1 \le M_n \le 10$). In order for each measurement to be weighted equally, glaciers with more

70 measurements receive greater weight than those with fewer measurements. Thus the
71 decadal mean for the data set is computed as

72 $$\bar{\alpha} = \frac{\sum_{n=1}^{N} f_n \bar{\alpha}_n}{N_f}, \quad (4)$$

73 where $f_n = M_n / 10$, $\bar{\alpha}_n$ is given by

74 $$\bar{\alpha}_n = \frac{\sum_{i=1}^{M_n} \alpha_{ni}}{M_n}, \quad (5)$$

75 and

76 $$N_f = \sum_{n=1}^{N} f_n . \quad (6)$$

77 Equation (4) is equivalent to the arithmetic mean of all measurements, with each
78 measurement weighted equally. We can think of N_f as the equivalent number of glaciers;
79 it is equal to the total number of measurements divided by the number of years. The
80 variance is given by

81 $$\sigma^2 = \frac{1}{N_f - 1} \sum_{n=1}^{N} f_n (\bar{\alpha}_n - \bar{\alpha})^2, \quad (7)$$

82 and the standard error is

83 $$\delta\alpha = \frac{\sigma}{\sqrt{N_f}}. \quad (8)$$

84 The arithmetic mean AAR and its standard error, shown in the second section of Sheet C
85 for 2001–2010 only, are computed analogously.

86 To assess the data for size biases, we plotted the mean value of α for each glacier
87 (Sheet C) against the log of glacier area (Sheet A). As shown in Fig. S2, the correlation is
88 slightly positive ($r^2 = 0.03$) but statistically insignificant ($p > 0.10$). The correlation
89 between α and glacier area (Sheet A) is also insignificant. A positive correlation between

90 glacier area and the change in α (relative to the equilibrium value of 1.0) would be
91 expected if (1) larger glaciers have greater elevation ranges than smaller glaciers, (2) for a
92 given lifting of the equilibrium line altitude (ELA), the AAR decreases less for glaciers
93 with large elevation ranges than for glaciers with small elevation ranges, and (3) the
94 average lifting of the ELA in a warming climate is independent of glacier size. The lack of
95 a significant correlation between glacier area and α suggests that one or more of these
96 assumptions does not apply to the observed GIC. We checked for area-range bias (i.e., a
97 violation of the first assumption) by comparing plots of glacier area vs. elevation range for
98 (1) the observed GIC and (2) more than 100,000 GIC in the World Glacier Inventory
99 (Cogley et al., 2009b). We did not find evidence of a significant bias.

100 The next sections of Sheet C show the 2001–2010 arithmetic mean values of p_A and
101 p_V for the full data set. BDM showed that for a given glacier or ice cap, $p_A = \alpha - 1$ and
102 $p_V = \alpha^\gamma - 1$, where $\alpha = \mathrm{AAR} / \mathrm{AAR}_0$ and γ is the exponent in the glacier volume-area
103 scaling relationship, $V = cA^\gamma$ (Bahr et al., 1997). Data and theory suggest $\gamma = 1.25$ for ice
104 caps and $\gamma = 1.36$ for glaciers. Thus p_V depends on γbut not on the poorly constrained
105 constant *c*, and p_A is independent of both *c* and γ. We compute means of p_A and p_V first for
106 glaciers, then separately for ice caps. (In the text below, we generally refer to "glaciers",
107 but the same analysis applies to ice caps with the appropriate value of γ.) For a single
108 glacier we have $\overline{p}_{An} = \overline{\alpha}_n - 1$ and $\overline{p}_{Vn} = \overline{\alpha}_n^\gamma - 1$, where $\overline{\alpha}_n$ is the mean value of α for
109 glacier *n* over the decade. Suppose we have at least one α value during the decade for
110 each of *N* glaciers. To give greater weight to glaciers with more measurements, we
111 compute the decadal mean $\overline{p}_A$ and $\overline{p}_V$ as

112 $$\overline{p}_A = \frac{\sum_{n=1}^{N} f_n \overline{\alpha}_n}{N_f} - 1 \qquad (9)$$

and

$$\overline{p}_V = \frac{\sum_{n=1}^{N} f_n \overline{\alpha_n^\gamma}}{N_f} - 1, \tag{10}$$

The variance associated with p_A is

$$\sigma_{p_A}^2 = \frac{1}{N_f - 1} \sum_{n=1}^{N} f_n (\overline{\alpha}_n - \overline{\alpha})^2, \tag{11}$$

and the variance associated with p_V is

$$\sigma_{p_V}^2 = \frac{1}{N_f - 1} \sum_{n=1}^{N} f_n (\overline{\alpha_n^\gamma} - \overline{\alpha^\gamma})^2. \tag{12}$$

The standard errors are

$$\delta p_A = \frac{\sigma_{p_A}}{\sqrt{N_f}} \tag{13}$$

and

$$\delta p_V = \frac{\sigma_{p_V}}{\sqrt{N_f}}. \tag{14}$$

If these data are taken to be globally representative, as assumed by BDM, then we compute that the Earth's glaciers must lose 44 ± 6% of their area and 51 ± 7% of their volume, and ice caps must lose 32 ± 9% of their area and 38 ± 10% of their volume, to reach equilibrium with the climate of the past decade. As discussed in the main text, however, these estimates may be geographically biased.

5. Pentadal mass balance calculations

Sheet D (*Pentadal mass balance*) shows pentadal average mass balances for the full data set during 1971–2010, with each mass-balance measurement weighted equally (Table S1).

6. High-mass regional calculations

Sheet E (*High mass regions*) is similar to sheet C, except that it includes only the 38 GIC in high-mass regions, defined as regions with a total GIC volume of at least 5,000 km^3 as estimated by Radić and Hock (2010). These regions are Arctic Canada, Antarctica, Alaska, Greenland, the Russian Arctic, Central Asia, Svalbard, and the Southern Andes. The first three sections show AAR, mass balance, and α, respectively. Decadal mean values of α, p_A, and p_V and the associated standard errors are shown in Sheet E. These are the "method 2" averages cited in the text. The arithmetic mean and 10-year running mean are shown in Fig. 3 of the main text, where the 40-year linear trend (1971–2010) and two 20-year linear trends (1971–1990 and 1991–2010) of the mean values are illustrated in Sheet E. We used a *t*-test to determine significance. The 1970–2009 and 1990–2009 trends are statistically significant at the 1% level, whereas the 1970–1989 trend is insignificant at the 10% level. In the last section of Sheet E, we repeated the annual mean and trend calculations for the 11 GIC in high-mass regions with observations in all four decades, to assess the effect on the trends of the changing composition of the data set. The trends are very similar to those computed for all 38 GIC.

The mean α is closely related to the mean mass balance. Figure S4 shows that the annual average mass balance values computed for the full data set of Sheet D are closely correlated ($r^2 = 0.82$) with the annual average α values of Sheet C. A similar high correlation ($r^2 = 0.75$) holds for the GIC in high-mass regions, with annual values of mass balance and α computed on Sheet E. A mass-balance decrease of 100 kg m^{-2} yr^{-1} is associated with a decrease of about 0.06 in α.

7. Regional mass balance calculations

158 Sheet F (*Regional mass balance*) shows the average mass balance during 2001–
159 2010 for each of 14 regions (Table S2), the estimated GIC area in the region (Radić and
160 Hock, 2010) and the corresponding fraction of the Earth's total GIC area. For the past
161 decade the data set has no observations from the Russian Arctic, which contains an
162 estimated 8% of global GIC area, or from North Asia, which contains much less than 1%.
163 For purposes of regional upscaling, we used Svalbard (which is climatically similar) as a
164 surrogate for the Russian Arctic, and we neglected North Asia. Thus the regional area
165 fractions are relative to a global total that omits the small GIC area in North Asia. The
166 global average mass balance is computed as

167 $$b_{\text{global}} = \sum_n w_{An} b_n, \tag{15}$$

168 where w_{An} is the fractional area weight for region *n*, and b_n is the mean mass balance.
169 Sheet F shows the global average mass balance computed for the full decade, for each of
170 two pentads, and for the period 2003–2010 (corresponding to Jacob et al. (2012)). To
171 convert the results of Jacob et al. (2012) to an area-average mass balance, we divided the
172 estimated mass loss of 148 ± 30 Gt yr^{-1} by an estimated GIC area (Radić and Hock, 2010)
173 of 511×10^3 km^2, excluding peripheral Greenland and Antarctic glaciers.
174

175 **8. Regional alpha calculations**

176 Sheet G (*Regional alpha*) shows regional mean values of α in 2001–2010 for the
177 same 14 regions (Table 1 in the main text). Again, Svalbard is used as a surrogate for the
178 Russian Arctic, and North Asia is neglected. Decadal mean α for each glacier and ice cap
179 are shown in Sheet G. Measurements of α were averaged, with each measurement
180 weighted equally, to obtain the regional means $\overline{\alpha}_n$. The estimated area and volume losses
181 per region are $\overline{p}_{An} = \overline{\alpha}_n - 1$ and $\overline{p}_{Vn} = \left(\overline{\alpha}_n\right)^{\overline{\gamma}_n} - 1$, where $\overline{\gamma}_n$ is estimated as described below.

The upscaled global estimates are obtained by summing over regions, with each regional value weighted by the estimated total GIC area in the region (for α and p_A) and total volume (for p_V):

$$p_{Aglobal} = \sum_n w_{An} \overline{p}_{An}, \tag{16}$$

$$p_{Vglobal} = \sum_n w_{Vn} \overline{p}_{Vn}. \tag{17}$$

The upscaled values, with errors, are shown in Sheet G. The regional area and volume weights, w_{An} and w_{Vn}, are also shown in Sheet G.

The errors for these global estimates are given by

$$\left(\delta p_{Aglobal}\right)^2 = \sum_n (w_{An} \delta p_{An})^2, \tag{18}$$

$$\left(\delta p_{Vglobal}\right)^2 = \sum_n (w_{Vn} \delta p_{Vn})^2, \tag{19}$$

where δp_{An} and δp_{Vn} are the regional errors. For each region we have $\delta p_{An} = \delta \alpha_n$, where $\delta \alpha_n$ (shown in column V) is estimated by the following method. We subsampled GIC in two well-represented regions, Central Europe and W. Canada/U.S. For 2001–2010 we considered $n = 15$ glaciers with continuous records in Central Europe, and $n = 14$ glaciers with continuous records in Western Canada/U.S. The full samples per region provide reference mean values of α for each region. For each region we computed means for all possible subsamples containing 1 to $n-1$ glaciers. We then plotted the difference between $\overline{\alpha}$ of each subsample and $\overline{\alpha}$ of the full sample (Fig. S3a). The spread of differences as a function of subsample size gives an estimate of $\delta \alpha_n$ in poorly sampled regions with small spatial area (Iceland, Svalbard, Northern Andes, Caucasus and New Zealand). For regions containing more than 10 glaciers with observed AAR (Central Europe, Scandinavia and European Alps) we assigned an error based on a subsample size of 12. All errors are derived as root-mean-square-errors, RMSE, at 95% confidence interval. Based on the data

from Central Europe, which has a wider spread of differences than W. Canada/U.S., the errors (values of *n* shown in parentheses) are: Iceland (10), $\delta\alpha = 0.09$; Svalbard (6), $\delta\alpha = 0.15$; Northern Andes (4), $\delta\alpha = 0.21$; Caucasus (2), $\delta\alpha = 0.32$; New Zealand (1), $\delta\alpha = 0.47$; Central Europe (19), Scandinavia (18) and W. Canada/U.S. (18), $\delta\alpha = 0.06$.

For poorly sampled regions covering large spatial area (Central Asia, Alaska, Antarctica, Arctic Canada, the Southern Andes, and Greenland), we carried out the same analysis but using two combined regions: (1) Central Europe and Scandinavia; and (2) W. Canada/U.S. and Alaska (Fig. S3b). Thus, in addition to $n = 15$ glaciers from Central Europe we included $n = 5$ glaciers from Scandinavia; and in addition to $n = 14$ glaciers from W. Canada/U.S. we included $n = 2$ glaciers from Alaska. For each of these two extended regions we carried out a correlation analysis and showed that time series of α are not significantly correlated when the distance between glaciers exceeds ~300 km (Fig. S5). Therefore, the glacier sampling in the combined regions is representative for poorly sampled regions covering large spatial area whose glaciers experience different climatic regimes within the region. Based on the data from Central Europe and Scandinavia (which has a wider spread of differences than W. Canada/U.S. and Alaska), the errors at 95% confidence interval (values of *n* shown in parentheses) are: Central Asia (7), $\delta\alpha = 0.16$; Alaska and Antarctica (3), $\delta\alpha = 0.28$; Arctic Canada (2), $\delta\alpha = 0.35$; Greenland and Southern Andes (1), $\delta\alpha = 0.51$.

Since p_V is a function of both α and γ, the regional errors δp_{Vn} depend on both $\delta\alpha_n$ and $\delta\gamma_n$:

$$(\delta p_{Vn})^2 = \left(\frac{\partial p_V}{\partial \alpha}\right)^2_{\bar{\alpha}_n} (\delta\alpha_n)^2 + \left(\frac{\partial p_V}{\partial \gamma}\right)^2_{\bar{\gamma}_n} (\delta\gamma_n)^2, \tag{20}$$

where $\bar{\alpha}$ and $\bar{\gamma}$ are best estimates. Evaluating the derivatives, this becomes

$$(\delta p_{Vn})^2 = \left(\bar{\gamma}_n\ \bar{\alpha}_n^{\bar{\gamma}-1}\right)^2 (\delta\alpha_n)^2 + \left(\bar{\alpha}_n^{\bar{\gamma}} \ln(\bar{\alpha}_n)\right)^2 (\delta\gamma_n)^2. \tag{21}$$

We estimated $\overline{\gamma}_n$ and $\delta\gamma_n$ as explained in the next section.

9. Glacier vs. ice cap partitioning

Drawing from existing glacier inventories (Cogley, 2009b), we tabulated the total number of GIC and the number of ice caps in each region (Table S3). Ice cap fraction numbers are also shown in Sheet H (*G vs. IC partition*). Regions with relatively few ice caps (less than 1% of the total number of GIC in the regional inventory) were assumed to have most of their volume contained in glaciers. For these regions we assumed $\overline{\gamma} = 1.36 \pm 0.02$, where the error corresponds roughly to the difference between the observed value of 1.36 for valley glaciers and the theoretical value (Bahr et al., 1997) of 1.375. For regions where at least 1% of the GIC are classified as ice caps, we assumed $\overline{\gamma} = 1.31 \pm 0.05$ to reflect an uncertain partitioning of volume between glaciers and ice caps. (Because ice caps can be much larger than typical glaciers, a relatively small number of ice caps can contain a substantial fraction of a region's volume. BDM, for example, estimated that 53% of total GIC volume is contained in ice caps and 47% in glaciers, although there are many more glaciers than ice caps.) A more complete analysis would use scaling relationships to estimate the total glacier and ice cap volume in each region. Existing inventories, however, do not contain complete lists of glaciers and ice caps in all regions, nor do all GIC fall clearly into one category or the other.

Although the partitioning between glaciers and ice caps is only approximate, our results are not sensitive to the details of this partitioning. The errors δp_{Vn} are dominated by the term containing $\delta\alpha_n$ (the first term on the RHS of Eq. (21)), with much smaller contributions from the term containing $\delta\gamma_n$ (the second term on the RHS of Eq. (21)).

10. Future mean alpha

To estimate future values of the global mean α, we took $\alpha_{global} = 0.70 \pm 0.10$ as a best estimate for 2005. We applied the 40-year trend (-0.0052 ± 0.0033 yr^{-1}) shown in sheet E for the 38 high-mass GIC (method 2). Extending this trend for 35 years gives a decrease of -0.18 ± 0.12, resulting in $\alpha_{global} = 0.52 \pm 0.16$ by 2040. We set $p_{V\text{global}} = \left(\overline{\alpha}_{\text{global}}\right)^{\overline{\gamma}} - 1$, with $\overline{\gamma} = 1.31 \pm 0.05$ to reflect an uncertain partitioning of volume between glaciers and ice caps. The error $\delta_{Pvglobal} = 0.17$ was calculated in analogy to Eq. (20):

$$(\delta p_V)^2 = \left(\frac{\partial p_V}{\partial \alpha}\right)^2_{\overline{\alpha}} (\delta\alpha)^2 + \left(\frac{\partial p_V}{\partial \gamma}\right)^2_{\overline{\gamma}} (\delta\gamma)^2. \quad (22)$$

11. Glacier volume response times

The volume response time for a glacier, defined as the time scale for exponential adjustment to a new steady-state volume following a mass-balance perturbation, can be estimated as $\tau_V \sim H / |b_T|$, where H is a thickness scale (e.g., mean glacier thickness) and b_T is the mass balance at the terminus (Jóhannesson et al., 1989). For typical glaciers with thicknesses of 100 to 500 m and terminus melt rates of 1 to 5 m yr^{-1}, the response time is on the order of 100 yr. The mean terminus melt rate for our data set is ~3 m yr^{-1}, as shown in Sheet I (*Terminus mass balance*).

Bahr and Radić (2012) showed that the fraction of total volume contained in glaciers of area less than $A_{\min}$ is given to a good approximation by

$$\Theta = \left(\frac{A_{\min}}{A_{\max}}\right)^{\gamma-\beta+1}, \quad (23)$$

where $A_{\max}$ is the area of the largest glaciers, $\gamma = 1.375$ is the exponent in the volume-area scaling relationship $V \propto A^{\gamma}$, and $\beta = 2.1$ is the exponent in the power law $N(A) \propto A^{-\beta}$,

which predicts the number of glaciers N of size A. Volume-area scaling implies $h \propto A^{\gamma-1}$, where h is the mean ice thickness. Therefore

$$\Theta = \left(\frac{h_{\min}}{h_{\max}} \right)^{\frac{\gamma-\beta+1}{\gamma-1}} . \quad (24)$$

The largest glaciers and ice caps have a thickness of about 1000 m. Setting $h_{\min}$ = 500 m and $h_{\max}$ = 1000 m in Eq. (24), we obtain $\Theta = 0.60$, implying that approximately 60% of total glacier volume resides in glaciers thinner than 500 m. This analysis suggests that glaciers with response times on the order of a century or less contain a majority of the Earth's total glacier volume.

12. Contributing investigators

The principal investigators for the glaciers and ice caps in the WGMS database are listed in WGMS (2012) and earlier bulletins. We have supplemented the WGMS database with data compiled by Mark Dyurgerov (Dyurgerov et al., 2005; Bahr et al., 2009). In addition, we thank the following investigators for providing us with data not previously in the WGMS database:

- Pedro Skvarca: *Bahia Del Diablo*
- Andrea Fischer and Gerhard Markl: *Hintereisferner, Jamtalferner, Kesselwandferner*
- Heinz Slupetzky: *Sonnblickkees*
- Ludwig N. Braun: *Vernagtferner*
- Reinhard Böhm and Wolfgang Schöner: *Goldbergkees, Klienfleisskees, Wurtenkees*
- Javier C. Mendoza Rodríguez and Bernard Francou: *Charquini Sur, Zongo*
- Alex Gardner: *Devon Ice Cap NW*
- Graham Cogley: *White*
- Bolívar Cáceres Correa and Bernard Francou : *Antizana 15 Alpha*

- Niels Tvis Knudsen: *Mittivakkat*
- Finnur Pálsson, Helgi Björnsson, and Hannes Haraldsson: *Brúarjökull, Eyjabakkajökull, Köldukvíslarjökull, Langjökull S. Dome, Tungnaárjökull*
- Þorsteinn Þorsteinsson: *Hofsjökull N, Hofsjökull E, Hofsjökull SW*
- Luca Carturan: *Carèser*
- Luca Mercalli: *Ciardoney*
- Gian Carlo Rossi and Gian Luigi Franchi: *Malavalle, Pendente*
- Bjarne Kjøllmoen: *Ålfotbreen, Breidalblikkbrea, Gråfjellsbrea, Langfjordjøkelen, Nigardsbreen*
- Hallgeir Elvehøy: *Austdalsbreen, Engabreen, Hardangerjøkulen*
- Liss M. Andreassen: *Gråsubreen, Hellstugubreen, Storbreen*
- Jack Kohler: *Austre Brøggerbreen, Kongsvegen, Midtre Lovénbreen*
- Piotr Glowacki and Dariusz Puczko: *Hansbreen*
- Ireneusz Sobota: *Waldemarbreen*
- O.V. Rototayeva: *Garabashi*
- Yu K. Narozhniy: *Leviy Aktru, Maliy Aktru, and No. 125*
- Miguel Arenillas: *Maladeta*
- Peter Jansson: *Mårmaglaciären, Rabots glaciär, Riukojietna, Storglaciären*
- Giovanni Kappenberger and Giacomo Casartelli: *Basòdino*
- Martin Funk and Andreas Bauder: *Gries, Silvretta*
- Mauri Pelto: *Columbia (2057), Daniels, Easton, Foss, Ice Worm, Lower Curtis, Lynch, Rainbow, Sholes, Yawning, Lemon Creek*
- Jon Riedel: *Noisy Creek, North Klawatti, Sandalee, Silver*
- Rod March and Shad O'Neel: *Gulkana, Wolverine*
- William R. Bidlake: *South Cascade*

326 **Supplementary Tables**

327

328 **Table S1.** Pentadal global mean mass balance (kg m^{-2} yr^{-1}), 1971–2010, for the updated
329 data set (methods 1 –3) and for Kaser et al. (2006) and Cogley (2012).

Method or published study	1971–1975	1976–1980	1981–1985	1986–1990	1991–1995	1996–2000	2001–2005	2006–2010
Kaser et al. (2006)	-90	-310	-237	-258	-286	-483	-510	
Cogley (2012)	-213	-414	-360	-338	-334	-526	-748	-487
Method 1 (all GIC)	-44	-195	-203	-245	-278	-365	-885	-708
Method 2 (high-mass regions)	-282	-330	-215	-201	-312	-428	-534	-386
Method 3 (regional upscaling)							-441	-429

Table S2. Regional mean mass balance and α for 2001–2010, with the number of observed GIC per region shown in parentheses.

Region	Mean mass balance (kg m^{-2} yr^{-1})	Mean α
Alaska (3)	-686	0.89
W. Canada/U.S. (19)	-989	0.57
Arctic Canada (2)	-275	0.60
Greenland (1)	-986	0.34
Iceland (10)	-1063	0.72
Svalbard (6)	-471	0.49
Scandinavia (18)	-826	0.53
Central Europe (19)	-905	0.47
Caucasus (2)	-271	0.81
Central Asia (7)	-538	0.80
Northern Andes (4)	-835	0.71
Southern Andes (1)	-207	0.71
New Zealand (1)	-152	0.92
Antarctic (3)	-131	0.89

334 **Table S3.** Estimated ice cap fraction for each
335 region, based on Cogley (2009b).

Region	Ice cap fraction
Alaska	0.001
W. Canada/U.S.	0.000
Arctic Canada	0.041
Greenland	0.167
Iceland	0.250
Svalbard/Russian Arctic	0.110
Scandinavia	0.018
North Asia	0.016
Central Europe	0.001
Caucasus	0.007
Central Asia	0.012
Northern Andes	0.006
Southern Andes	0.010
New Zealand	0.000
Antarctic	0.255

Supplementary Figures

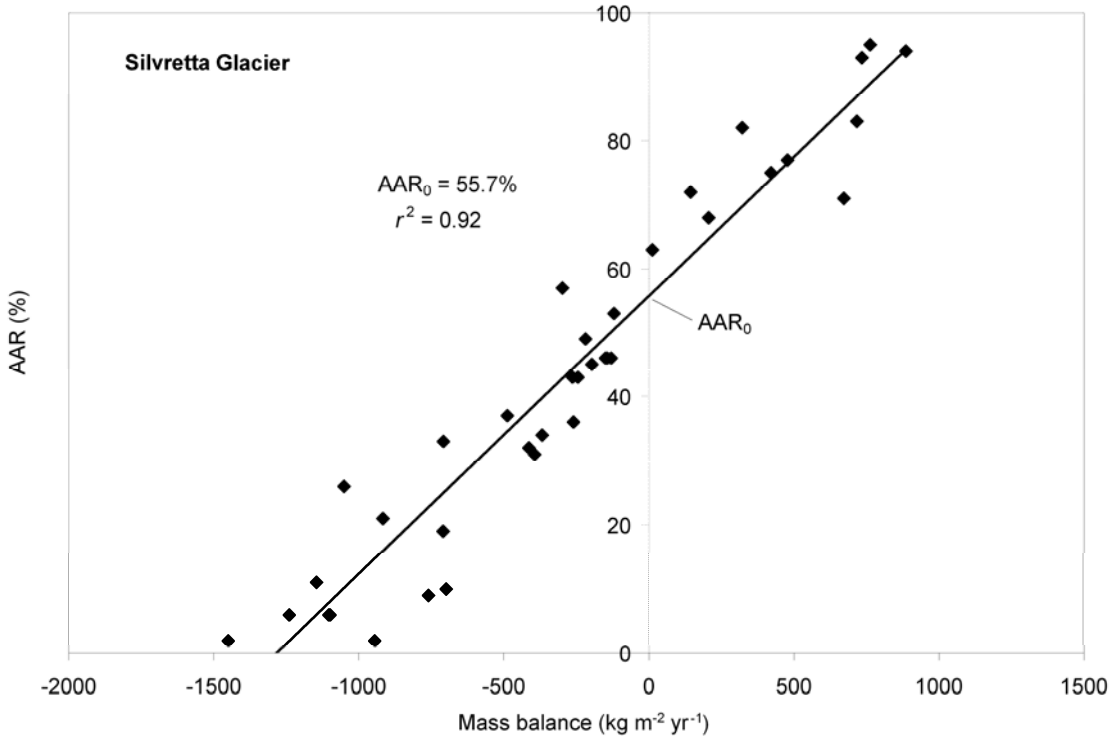

Fig. S1. Linear regression of AAR against mass balance for Silvretta glacier. The *y*-intercept is AAR_0, the equilibrium value of AAR. Each diamond represents one year of data.

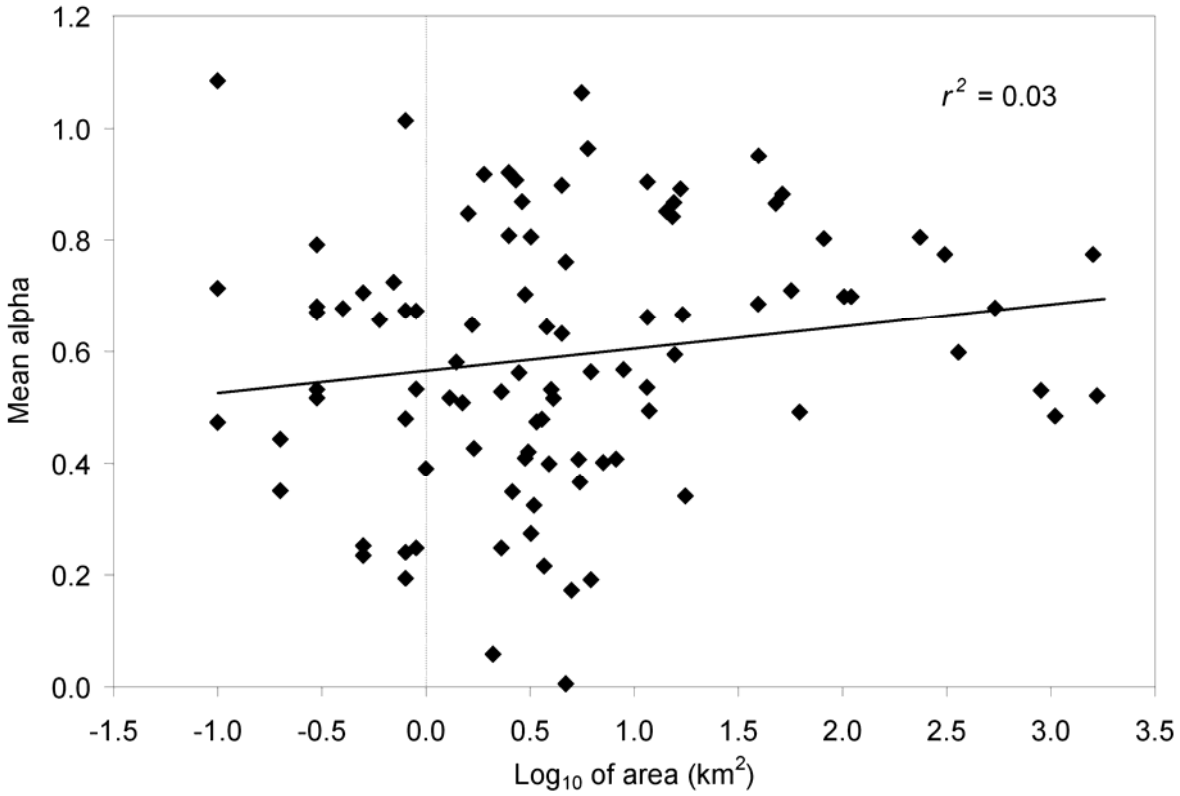

346

347

348 **Fig. S2.** Linear relation between the log of area (km^2) and the 2001–2010 mean

349 $\alpha = AAR/AAR_0$ for 96 GIC with observations in the past decade. Each diamond

350 represents one glacier or ice cap. The correlation between α and the log of area, although

351 slightly positive ($r^2 = 0.03$), is insignificant ($p > 0.10$), suggesting that a bias toward

352 smaller glaciers does not imply a bias in α.

353

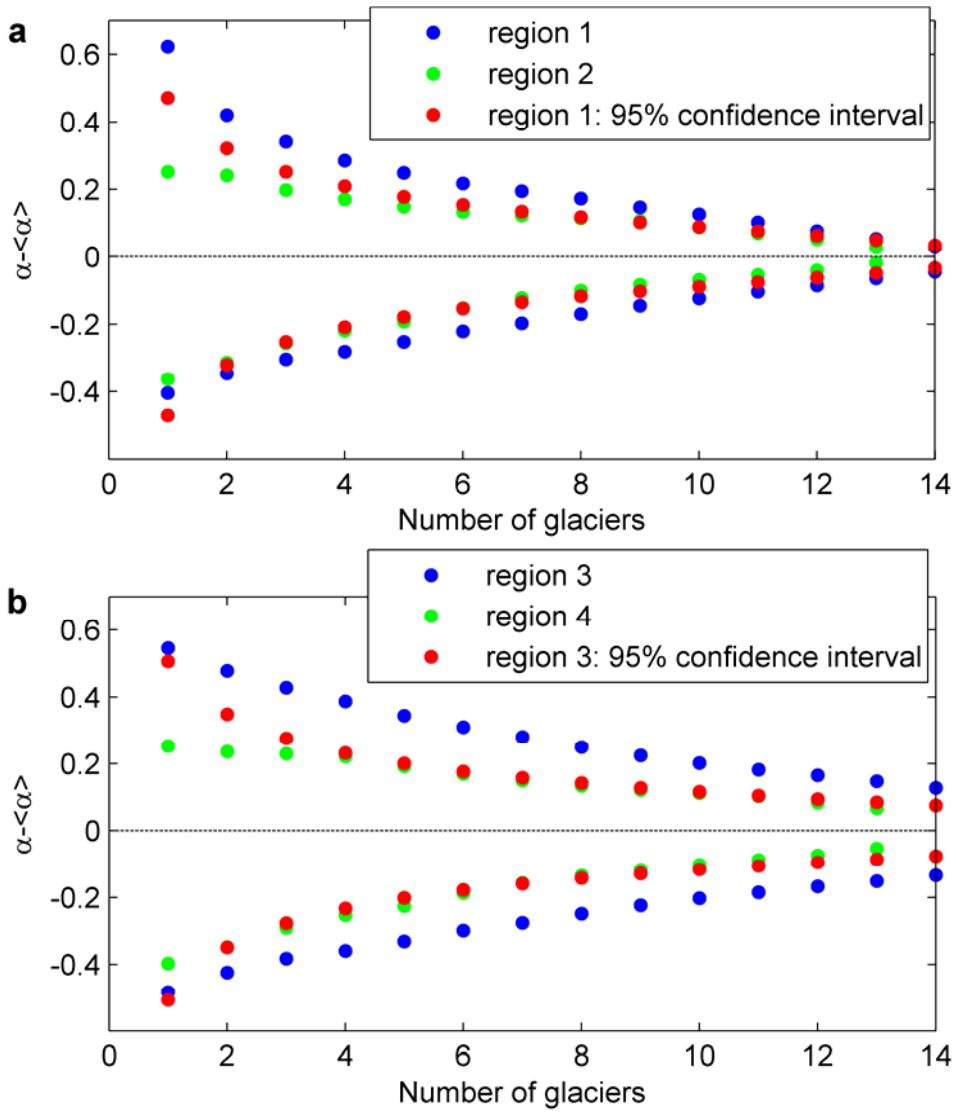

354

355

356 **Fig. S3.** Spread of decadal mean α as a function of subsample size in well-sampled

357 regions. This plot shows the maximum difference between subsample mean α and

358 reference $\langle\alpha\rangle$ as a function of the number of glaciers in the subsample for: (a) two well-

359 sampled regions, region 1: Central Europe and region 2: W. Canada/U.S, and (b) the same

360 regions but extended, region 3: Central Europe and Scandinavia and region 4: W.

361 Canada/U.S. and Alaska. The reference $\langle\alpha\rangle$ is the mean of the full sample, which includes

362 glaciers with continuous AAR series during 2001–2010. In red is the difference range at

363 95% confidence interval (1.96 × standard deviation) from region 1 and region 3.

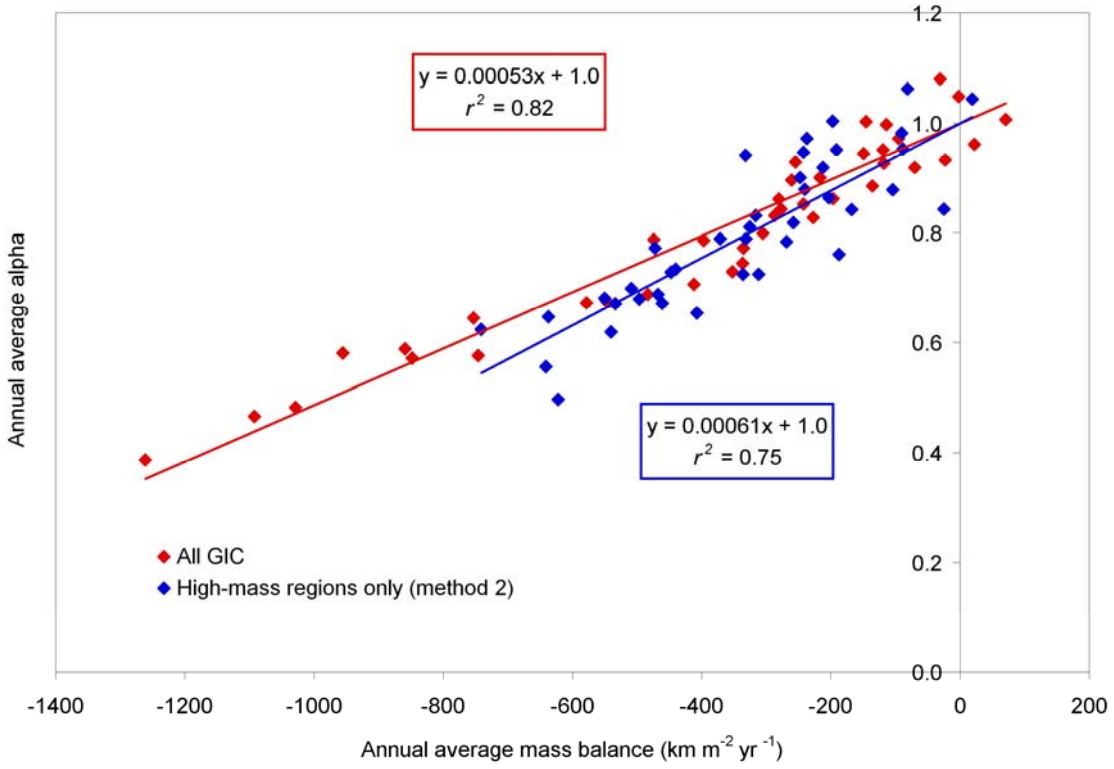

Fig. S4. Linear relation between average mass balance and average α, 1971–2010. Each diamond represents the average of all GIC observations for one year. The red diamonds denote averages over the full data set, and the blue diamonds denote averages over the GIC in high-mass regions only. The regression line is forced to pass through the point $y = 1.0$. Both correlations are significant ($p < 0.01$), as determined from the squared correlation coefficient, r^2. A change in mass balance of 100 kg m^{-2} yr^{-1} is associated with a change in α of about 0.06.

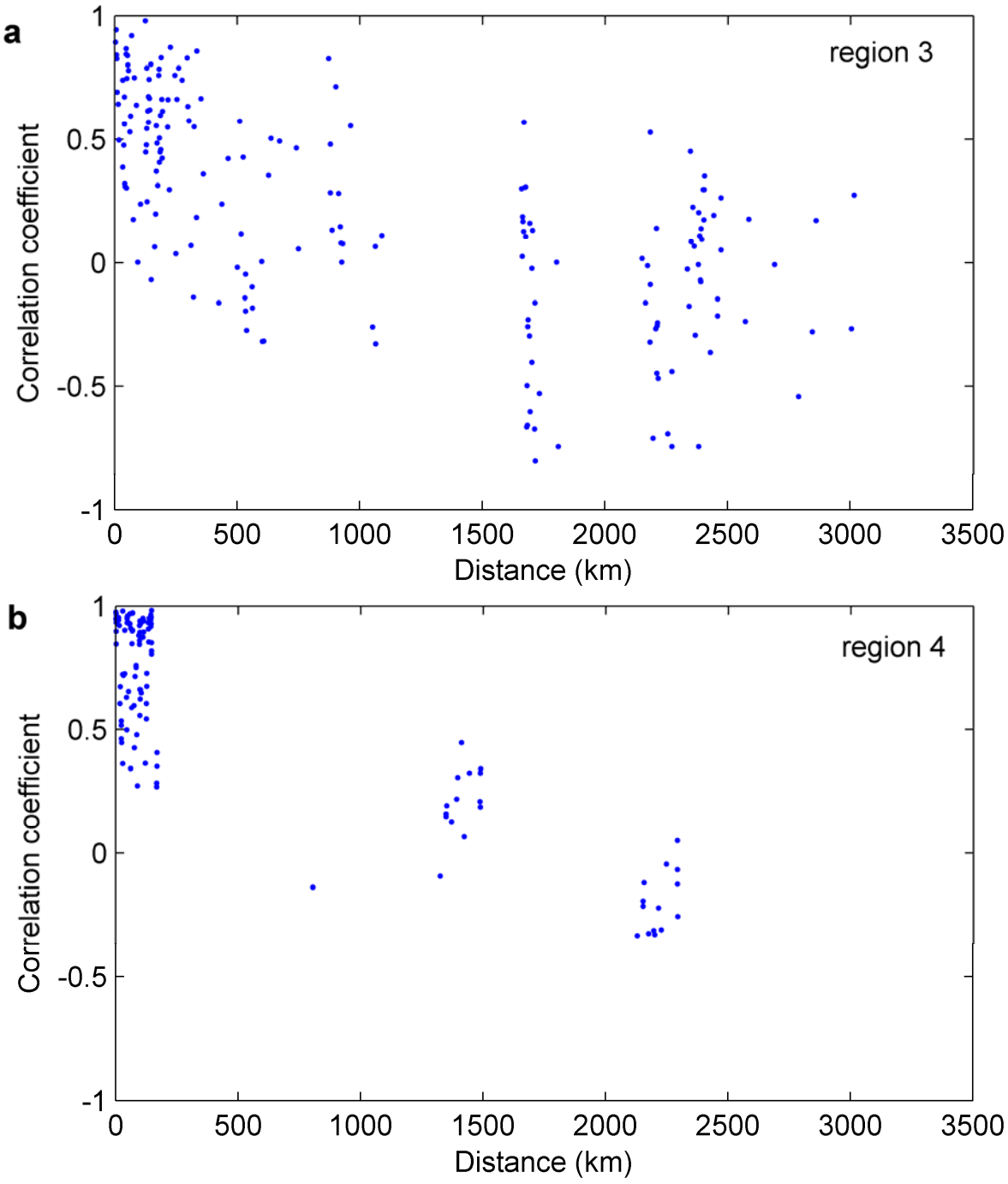

Fig. S5. Correlation between α time series (2001–2010) of any two glaciers in a region versus the distance between the two glaciers. (a) Region 3: Central Europe (15 glaciers) and Scandinavia (5 glaciers), (b) region 4: W. Canada/U.S. (14 glaciers) and Alaska (2 glaciers).